REPORT

An intelligent spinal soft robot with self-sensing adaptability

Shoulu Gong,[1,2,4] Fuyi Fang,[1,4] Zhiran Yi,[1,*] Bohan Feng,[2] Anyu Li,[2] Wenbo Li,[3] Lei Shao,[2,*] and Wenming Zhang[1,*]
*Correspondence: yizhiran@sjtu.edu.cn (Z.Y.); lei.shao@sjtu.edu.cn (L.S.); wenmingz@sjtu.edu.cn (W.Z.)
Received: December 13, 2023; Accepted: May 15, 2024; Published Online: May 21, 2024; https://doi.org/10.1016/j.xinn.2024.100640

GRAPHICAL ABSTRACT

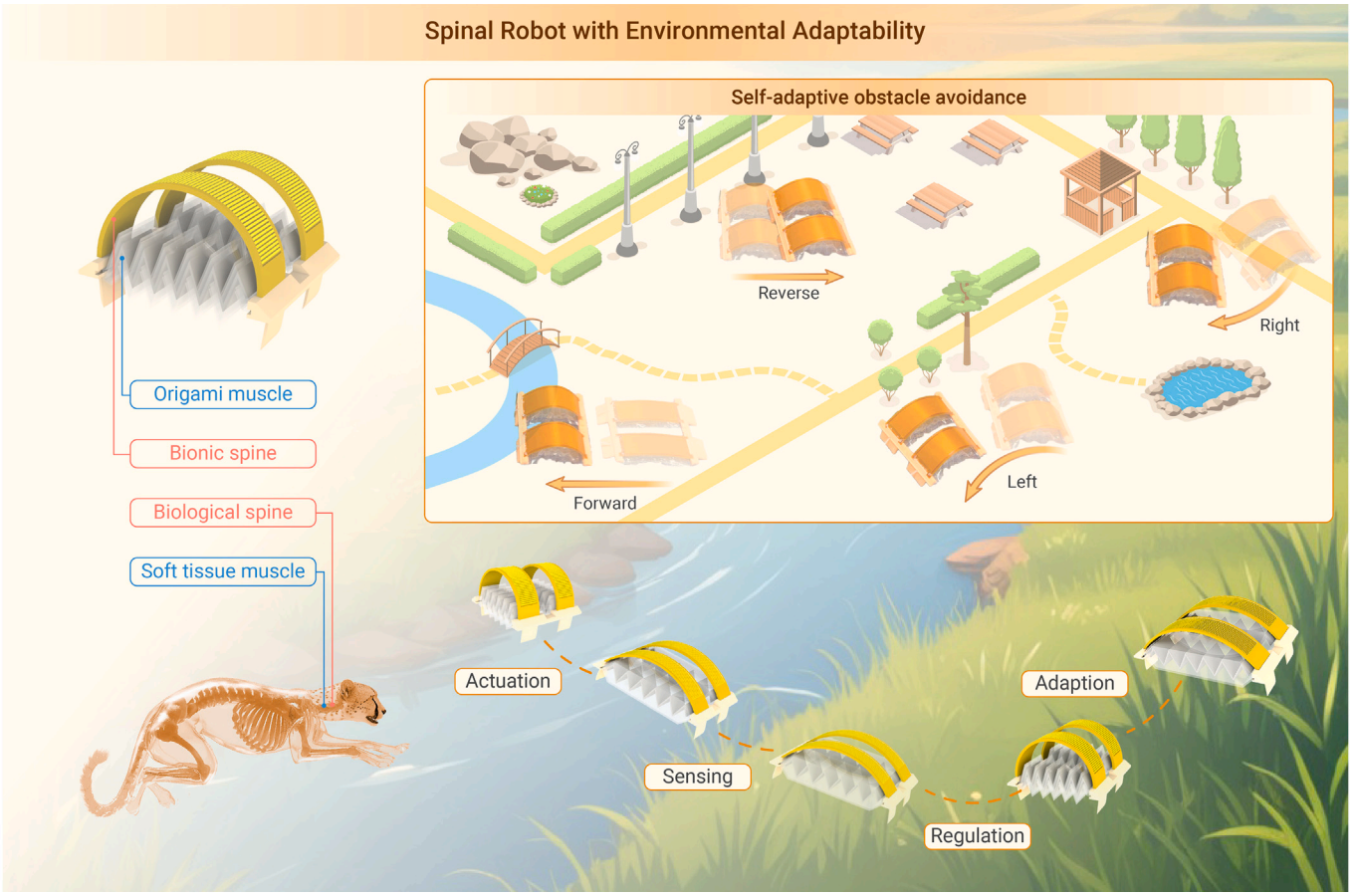

PUBLIC SUMMARY

- Intelligent spinal robots coupling sensing, recognition, and active adaption.
- A bionic spine with integrated sensing and actuation in one shared device.
- A design concept highly scalable for various robots for active environmental adaption and obstacle avoidance purposes.

REPORT

An intelligent spinal soft robot with self-sensing adaptability

Shoulu Gong,[1,2,4] Fuyi Fang,[1,4] Zhiran Yi,[1,*] Bohan Feng,[2] Anyu Li,[2] Wenbo Li,[3] Lei Shao,[2,*] and Wenming Zhang[1,*]

[1]State Key Laboratory of Mechanical System and Vibration, School of Mechanical Engineering, Shanghai Jiao Tong University, Shanghai 200240, China

[2]University of Michigan-Shanghai Jiao Tong University Joint Institute, Shanghai Jiao Tong University, Shanghai 200240, China

[3]School of Aerospace Engineering and Applied Mechanics, Tongji University, Shanghai 200092, China

[4]These authors contributed equally

*Correspondence: yizhiran@sjtu.edu.cn (Z.Y.); lei.shao@sjtu.edu.cn (L.S.); wenmingz@sjtu.edu.cn (W.Z.)

Received: December 13, 2023; Accepted: May 15, 2024; Published Online: May 21, 2024; https://doi.org/10.1016/j.xinn.2024.100640

Citation: Gong S., Fang F., Yi Z., et al., (2024). An intelligent spinal soft robot with self-sensing adaptability. The Innovation **5(4)**, 100640.

Self-sensing adaptability is a high-level intelligence in living creatures and is highly desired for their biomimetic soft robots for efficient interaction with the surroundings. Self-sensing adaptability can be achieved in soft robots by the integration of sensors and actuators. However, current strategies simply assemble discrete sensors and actuators into one robotic system and, thus, dilute their synergistic and complementary connections, causing low-level adaptability and poor decision-making capability. Here, inspired by vertebrate animals supported by highly evolved backbones, we propose a concept of a bionic spine that integrates sensing and actuation into one shared body based on the reversible piezoelectric effect and a decoupling mechanism to extract the environmental feedback. We demonstrate that the soft robots equipped with the bionic spines feature locomotion speed improvements between 39.5% and 80% for various environmental terrains. More importantly, it can also enable the robots to accurately recognize and actively adapt to changing environments with obstacle avoidance capability by learning-based gait adjustments. We envision that the proposed bionic spine could serve as a building block for locomotive soft robots toward more intelligent machine-environment interactions in the future.

INTRODUCTION

Soft robots are promising for agile locomotion and high-level intelligence like living creatures and have been developed in a wide range of applications, including human-machine and machine-environment interactions.[1-6] It is worth noting that among living creatures, vertebrate animals not only feature highly developed muscular and skeletal systems but also an advanced central nervous system enclosed within the spines, which helps them to react very quickly to changes in their surroundings. This gives them a competitive edge compared to most invertebrates, which behave almost entirely by instinct and with little capability to learn from their mistakes. Such sophisticated musculoskeletal and nervous systems supported by the spines endow vertebrates the exceptional capacity to choose the optimal solutions and execute adaption when facing different survival environments.

There has recently been a great amount of research effort to develop intelligent adaption capabilities in biomimetic soft robots. Distinguished from the environmental adaption capabilities[7-11] that have been developed in current soft robots, such as simple phototaxis effect and non-perceptual adaption via shape morphing,[12,13] the environment adaption of vertebrates encompasses the entire process of perceptual feedback and autonomous adaption, which is a typical representation of high-level biological intelligence[14-16] by long-term evolution. Such adaption mainly relies on two functions of the biological spine: one the perception capability based on the enclosed central nervous systems and the other the regulatory adaption capability supported by the musculoskeletal systems. This high-level intelligence is the key to higher task success rate and efficiency. Therefore, to achieve such a level of intelligence in soft robots, it is highly desired to construct an entirely sensor-actuator-integrated spinal soft robotic system.

Current research effort about sensor-actuator-integrated soft robots mainly focuses on sensing based on e-skins[17-20] or visual systems[21-26] with applications in surrounding detection (e.g., pH, ion, oil, blow flow, etc.),[27-34] self-body perception (e.g., physical interaction monitoring, self-motion monitoring, etc.),[35-39] and intelligent recognition (e.g., environmental awareness, objects classification, etc.).[40-44] However, these existing sensor-actuator integration strategies only provide soft robotic systems with a perception capability but with unsatisfactory improvement on their motional performance and adaptability for various environments,[14,15,45] because their sensor and actuator components are discrete and independent devices with inadequate synergistic and complementary interaction.[46-48] Challenges remain in achieving an expected high-level intelligence where soft robots could be aware of the environmental terrains from attempted locomotion and then make self-adjustments autonomously, followed by learning and memorization.

This study proposes an intelligent soft robot with a sensing-actuation-integrated unibody spine for environmental recognition and active adaption. A flexible piezoelectric macro-fiber composite sheet is developed as a bionic spine, acting as the core component built upon an origami pneumatic robot. This bionic spine works as the nexus between environmental awareness and active adaption based on two reversible physical effects (shown in Figure 1A) that are successfully decoupled by a full bridge circuit. For one thing, the piezoelectric effect of the bionic spine provides reliable sensing for different environmental terrains as back-action; for another, the auxiliary actuation functions of the bionic spine enhance the actuation performance of the pneumatic artificial muscles by the converse piezoelectric effect, allowing the soft robot to travel more efficiently in various environments. Hence, the proposed soft robotic system enables both environmental recognition and autonomous adaption capabilities, showing higher task success rate and efficiency. In the following sections, we elaborate on the design of the spinal soft robots, characterize their motion enhancement, and then show the process of environmental recognition by machine learning. Finally, we demonstrate that the robot can perform various highly efficient and even beyond-biological locomotion with self-sensing adaptability, such as multi-terrain transitions, autonomous obstacle avoidance, and self-adaptive amphibious motions, which stand out from all previous sensor-actuator-integrated soft robots.

RESULTS

Design and methodology

As shown in Figure 1B, the robot structure contains an origami pneumatic actuator as the soft artificial muscle, a piezoelectric macro-fiber composite sheet as the bionic spine, and two printed resin robot feet. The origami actuator is vacuum driven with several advantages, including light weight, easy manufacturing, and large linear contraction rate (Figure S2 and Text S1). The bionic spine serves for both actuation and sensing purposes. It can be utilized as a supporting and auxiliary actuation based on converse piezoelectricity to enhance the motion performance over different environments, while it can also be utilized as a robotic e-skin simultaneously. The feedback signals of the bionic spine based on direct piezoelectric effect are available for analyzing both the motion states and the environmental interactions of the robot.

The self-sensing adaption process between the robot and the environment can be divided into three stages. Below, we take the amphibious transition of the robot between the land and the aquatic area as an example. During stage (1), the motion states of the robot and its interaction with the environment are constantly monitored by the bionic spine; in stage (2), changes in the monitored feedback signals are detected during terrain change and utilized for terrain recognition based on a pre-trained machine learning model; in stage (3), the actuation state of the robot will be self-regulated to actively adapt to the newly recognized terrain, thus switching to an optimal motion solution for this task. To achieve such an adaption, both enhanced actuation efficiency and accurate terrain recognition are necessary. Most importantly, a bridge circuit is developed to eliminate the crosstalk inside the bionic spine between the feedback signal as a sensor and the excitation signal as an auxiliary actuation, finally realizing the proposed unibody sensor-actuator integration design (more in Text S3).

Characterization of the spinal auxiliary actuation

As shown in Figure 2A, we first construct a soft crawling robot using a single pneumatic artificial muscle to demonstrate the design concept of the bionic

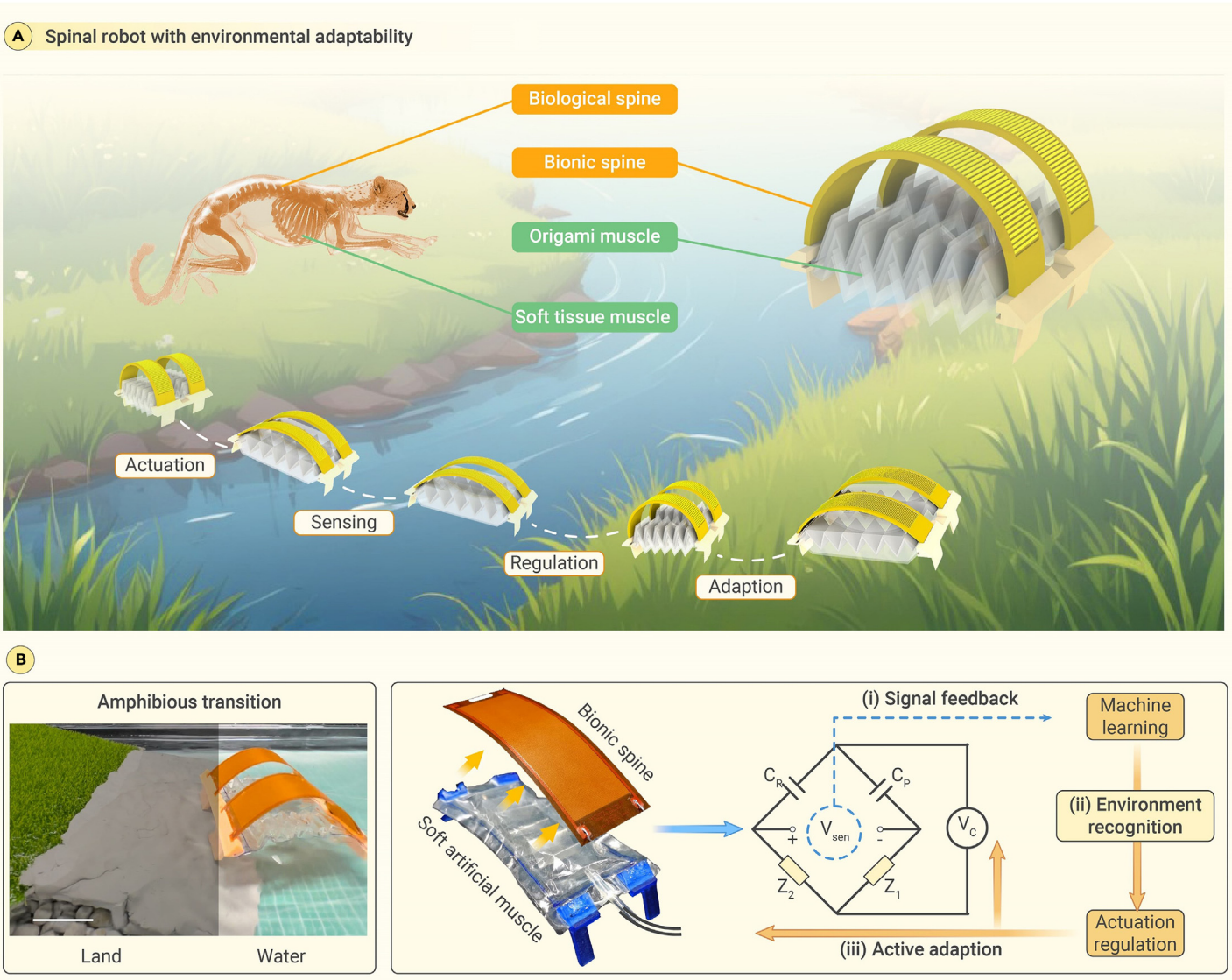

Figure 1. Depiction of high-level intelligence in both living creatures and soft robots (A) Spines for self-sensing, regulation, and environmental adaption. Vertebrate animals rely on spines for sensing and supporting and muscles for actuation. Proposed soft robots rely on bionic spines for sensing, support, and auxiliary actuation and origami muscles for actuation. (B) Demonstration of an autonomous self-sensing adaption process and methodology on the decoupling mechanism of a unibody sensing-actuation-integrated spine. Scale bar: 5 cm.

spine. The pneumatic actuation of the soft robot consists of two stages (more in Figure S6 and Text S1). First, when a negative pressure is applied, the artificial muscle contracts, and the deflection of the bionic spine increases, causing a simultaneous increase of the potential energy in both the bionic spine and the PET plastic skeleton inside the artificial muscle. As a result, the crawling robot will transit from the initial state to a contracted state. Second, when the negative pressure is withdrawn and a voltage is applied to the bionic spine to act as an auxiliary actuation, the crawling robot will revert to the initial state. The amplitude of the actuation pressure is set at −50 kPa to ensure dynamic stability of this soft crawling robot at different actuation frequencies. During the second stage, the potential energy of the PET plastic skeleton and bionic spine is released, leading to the generation of recovery forces $F_{Elastic}$ and $F_{Release}$ (more detail in Text S1), which can be expressed as follows:

$$F_{Elastic} = C_1 - C_2 x_a \quad \text{(Equation 1)}$$

$$F_{Release} = K_1 \left[\int_0^{\frac{\pi}{2}} \frac{d\varphi}{\sqrt{1 - sin^2 \frac{\partial}{2} sin^2 \varphi}} \right]^2 \quad \text{(Equation 2)}$$

As a result, the output force $F_{Auxiliary}$ generated by the bionic spine further facilitates the transition between the two motion states of the crawling robot, which can be expressed by the following equation:

$$F_{Auxiliary} = K_2 \frac{V}{y_a + \frac{x_a}{tan\partial}} \quad \text{(Equation 3)}$$

In the above equations, ∂ represents the central angle of the bent spine in a shape of a circularly arc, which significantly influences all output forces, C_1 and C_2 contain the intrinsic properties (sizes and Young's modulus) of the origami skeleton, K_1 and K_2 contain the properties (sizes, Young's modulus, and piezoelectric strain constant) of the bionic spine, x_a and y_a portray the shape of the curved bionic spine, and V is the applied voltage to the piezoelectric spine. Detailed derivations and modeling are available in Equations S1–S29.

The overall actuation force available in the second dynamic stage affects the crawling stride length of the robot. As an essential constituent of the overall actuation strategy, the auxiliary actuation is based on the converse piezoelectric effect of the bionic spine, and thus the amplitude of $F_{Auxiliary}$ is directly related to the magnitude of the excitation voltage. Figure 2B shows the normalized force amplitude of the soft crawling robot from the contracted state to the initial state (with a pneumatic actuation frequency of 1 Hz) as a function of the excitation voltage from 0.4 kV to 1 kV at the excitation frequencies of 1 Hz, 5 Hz, and

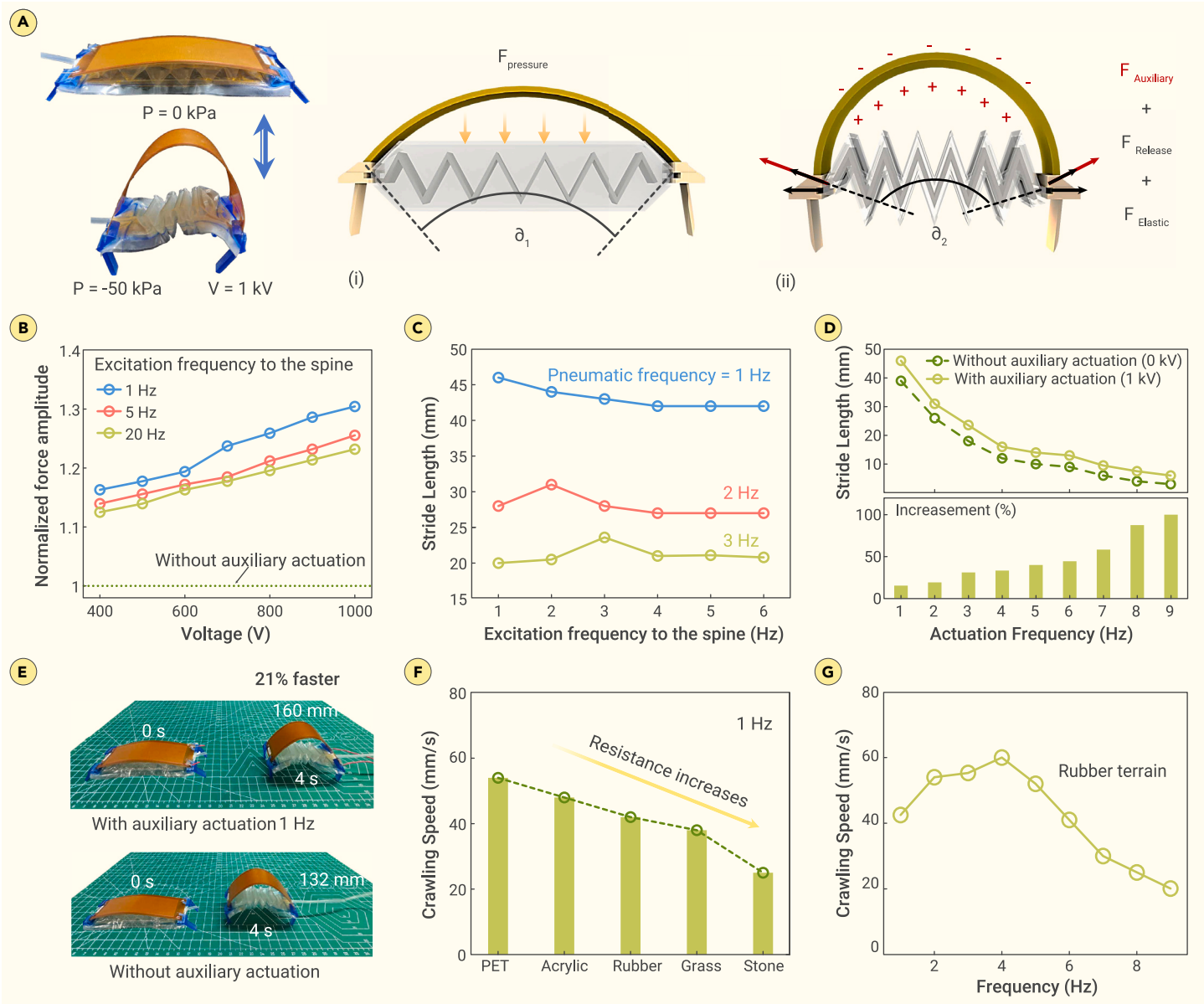

Figure 2. Actuation mechanism and characterization results of the spine-assisted actuation (A) Illustration of the actuation mechanism. (i) Contraction of the artificial muscle under vacuum pressure; (ii) recovering under the elastic force, release force, and auxiliary force generated by the artificial muscle and bionic spine. (B) Normalized recovery force under auxiliary actuation as a function of actuation voltage and actuation frequency, i.e., 1 Hz, 5 Hz, and 20 Hz from top to bottom, with the pneumatic actuation at 1 Hz. (C) Measured stride length of the crawling robot without terrain contact as a function of auxiliary frequency for three different pneumatic actuation frequencies, i.e., 1 Hz, 2 Hz, and 3 Hz. (D) Measured stride length of the robot as a function of actuation frequency with and without auxiliary actuation while the auxiliary voltage is 1 kV. (E) Comparison of robot crawling speed with and without auxiliary actuation on the rubber land. (F) Measured crawling speed of the robot at an actuation frequency of 1 Hz for different terrains. (G) Measured crawling speed of the robot as a function of actuation frequency on the rubber land.

20 Hz. The experimental results demonstrate that the presence of the auxiliary actuation greatly increases the overall output force in the second stage by approximately above 10%. The effectiveness of the auxiliary actuation increases linearly with voltage amplitude at a growth rate of approximately 1% per 0.1 kV, and the output force also performs with a similar trend at different excitation frequencies.

To achieve a synergistic mechanism between the auxiliary actuation of the bionic spine and the pneumatic actuation of the artificial muscle, we further optimize the actuation parameters. We first explore the association between different actuation parameters and the stride length of the crawling robot. Figure 2C shows the measured stride length of the crawling robot without terrain contacts as a function of the excitation voltage frequency for three different pneumatic actuation frequencies, 1 Hz, 2 Hz, and 3 Hz, indicating that the maximum stride length always occurs at the condition when the pneumatic and the auxiliary actuations are at the same frequency. In contrast to purely pneumatic actuation, the crawling robot with synergistic actuation outperforms by more than 20% in the stride length for the frequencies from 1 Hz to 9 Hz, as shown in Figure 2D. Moreover, the increments in stride lengths are especially pronounced (over 50%) when the actuation frequency exceeds 3 Hz, which is mainly because the auxiliary actuation force $F_{Auxiliary}$ greatly compensates the response hysteresis and low output force of the pneumatic artificial muscle at high frequencies. Figure 2E shows that the crawling robot with the auxiliary actuation has a 21% speed improvement from 33 mm/s to 40 mm/s moving on a green cutting board (a rubber-surfaced terrain). We note that although the auxiliary actuation could improve the locomotion speed, the actual crawling speed is still determined by both its dynamic states and the topographic characteristics of the contacting terrains.

Crawling speed of the robot on different terrains is a function of the actual stride length and actuation frequency. In general, both large motion stride length and high actuation frequency are beneficial for a faster locomotion but cannot be easily achieved simultaneously because the actuation frequency of the robot is inversely proportional to its stride length. Meanwhile, the resistance of the environmental terrain could reduce the stride length, causing a great variance of the crawling speed on different terrains. Figure 2F shows the measured crawling

speed with a synergistic actuation frequency of 1 Hz on different terrains, PET plastic, acrylic, rubber, grass, and stone from left to right while with increasing resistance in order (roughness from 10 μm to 3,000 μm), indicating a significantly varied crawling speed. It is important to understand that the effect of the contact resistance on locomotion speed is not always negative. For instance, a properly large contact resistance can actually prevent slipping, which greatly improves the crawling speed of the robot under high-frequency actuation. Hence, we consider that for each specific terrain, there is always a corresponding set of optimal actuation parameters for a better efficiency and a higher speed, such as the actuation frequency mentioned in this section. As shown in Figure 2G, the robot demonstrates the highest crawling speed with an optimal actuation frequency of 4 Hz on the rubber land, which is about 39.5% faster than the speed under 1 Hz. With similar experimental steps, we also obtained the optimal actuation frequency of the crawling robot on other terrains, including grass land, stone land, gravel land, PET land, plush land, and acrylic land (Figure S7), and these optimal actuation frequencies bring significant speed improvement ranging from 39.5% to 80% for the aforementioned terrains (Table S1). We believe that the robot possesses the potential to always maintain efficient motion over different terrains if knowing the type of the terrains beforehand, which could be achieved by combining sensing and autonomous adjustment.

Environment sensing and recognition by the spine

Regarding highly desired perception, the bionic spine endows this soft crawling robot with a self-sensing capability for both proprioception and exteroception using the decoupled piezoelectric feedback signal by the bridge circuit. We first demonstrate the proprioception capability of the robot by monitoring the feedback signal from the bionic spine during motion cycles under different actuation frequencies. As shown in Figure 3A, the measured signal can intuitively provide feedback on the change in crawling frequency and stride length. The motion states of the crawling robot can be then reconstructed based on the proposed model relating the responsive signal and the spinal bending angles (Figure S8 and Text S2), thus providing the crawling robot with the awareness of the position and movement of its own body.

In the above discussion, we have tested the relationship between the actual stride length of the crawling robot and the terrain resistance (more in Figure S7). As shown in Figure 3B, for some relatively smooth terrains, the difference in resistance can be observed by small features of the spinal feedback signal. For other terrains with uneven surface structures, the topographic differences expressed in the spinal feedback signal are much more pronounced (more in Figure S10). Thus, the exteroception capability of the crawling robot for different terrains can be realized by analyzing features in the feedback signal, including plush, grass, stone, gravel, acrylic, and rubber lands, as shown in Figure 3C.

To distinguish the proprioception and the exteroception information in the same piezoelectric signal, machine learning techniques are utilized in processing the feedback signal for further robot self-learning and adaption. The whole modeling and prediction process is shown in Figure 3D (more detail in materials and methods). Figure 3E shows that seven terrains with different roughness and morphology can be recognized with a high accuracy of 98.5% by the crawling robot based on the bionic spine and machine learning techniques. To validate the reliability of the trained learning model, the crawling robot is set to crawl continuously across multiple terrains while different kinds of multi-terrain combinations are used (Figure S11). The crawling robot shows a high identification accuracy of 97.1% for multi-terrain tasks (Figure 3F).

Multi-terrain active adaption of the soft spinal robot

With the well-trained machine learning network, the intelligence of the soft spinal robot is further illustrated by demonstrating its self-sensing adaptability to different terrains. Adaption means that the robot can always perform with optimal motion efficiency over different terrains, which is significant for crawling robots in the wild. More important, it greatly improves the success rate of the crawling robot to cope with multi-terrain tasks, where it may fail to move over changing terrains without autonomous adaption. Below, we show the superiority of the self-adaptive crawling robot by comparing its performance with a unimodal one under multi-terrain tasks.

The first task contains three terrains, which are rubber, stone, and PET plastic lands representing elastic, rough, and slippery conditions in sequence. We record the whole process of the crawling robot performing the tasks while monitoring the readouts of its bionic spine (Figure S12B). As shown in Figure 4A, the unimodal crawling robot passes the rubber land smoothly from 0 s to 4 s (with a fixed actuation frequency of 4 Hz, which is the optimal motion frequency for the crawling robot on the rubber terrain), but it failed to deal with the transition from the rubber land to the stone land. This failure is mainly due to the low output force and small stride length of the unimodal crawling robot at the frequency of 4 Hz, which prevents the robot from crossing the obstacle of the stone land. In contrast, the crawling robot with self-sensing adaptability can accomplish this task easily (Figure 4B and Video S1), and the whole process can be divided into three stages in time sequence. (1) From 0 s to 4 s, the robot passes the rubber land with an actuation frequency of 4 Hz; (2) from 5 s to 11 s, the robot arrives at the intersection of two terrains, and then the robot detects the terrain change and adjusts the actuation frequency from 4 Hz to 1 Hz itself to generate larger output force and stride length according to the result of pre-trained learning model; (3) from 12 s to 22 s, the robot passes the stone land and the PET land smoothly with a self-adjusted frequency of 1 Hz.

The second task contains grass land, plush land, and gravel land in sequential order. As shown in Figure 4C, the unimodal crawling robot takes 28 s to pass all three terrains with a fixed actuation frequency of 1 Hz. In reality, this performance could be a lot worse because we set the frequency at 1 Hz as we already knew it provides the highest efficiency on both grass and gravel lands. We then show that the crawling robot with self-sensing adaptability can finish the same task more efficiently (Figure 4D and Video S2). The whole process can also be divided into three steps in time sequence. (1) From 0 s to 5 s, the robot passes the grass land with an actuation frequency of 1 Hz; (2) from 6 s to 13 s, the robot arrives at the plush land, and then the robot changes its motion mode from 1 Hz to 6 Hz itself for optimal efficiency based on the bionic spine feedback (Figure S12D); (3) from 14 s to 23 s, the robot arrives at the gravel land and again changes its motion mode from 6 Hz back to 1 Hz itself to adapt to the gravel terrain. In this task, the robot equipped with self-adaption crawls over the plush land faster than the unimodal robot by 30%. Thus, the experimental results intuitively show that the proposed self-adaptive crawling robot can actively adapt to the terrain changes and maintain high motion efficiency by autonomous regulation.

Different from other soft robots or living creatures, the self-sensing adaptability of this robot is not dependent on visual feedback, and thus, it has a higher application potential than some living creatures. This spinal sensing strategy makes it possible for the robot to operate all day long in nature regardless of environmental brightness (Figure 4E). To further illustrate this beyond-biological intelligence, we demonstrate the self-adaptive motion of the crawling robot in dazzling lighting conditions and purely dark conditions. Figure 4F shows the crawling robot moving across a multi-terrain pathway under a dazzling lighting condition (Video S3). The monitored spinal feedback signal during this process is shown in Figure S13B, which intuitively reflects the motion states of the crawling robot and the terrain type at different moments. In this experiment, the crawling robot accomplishes self-adaptive motion over different terrains to select an optimal efficiency, with no assistance from vision feedback. Figure 4G also shows that the robot can perform self-adaptive motion for another multi-terrain pathway in purely dark conditions (Figure S13D and Video S4).

An amphibious omnidirectional robot

For broader application scenarios, we construct an amphibious soft robot by combining two spinal actuators as building blocks in parallel like a catamaran (Figure 5A). The two actuators could be driven separately to enable more complex overall motions. Based on a special robotic foot design and a sequential actuation of the left and right legs, the robot can realize nearly omnidirectional motions (more in Text S4). As shown in Figure 5B, when we drive the two robotic legs to move at the same actuation frequency, the motion of the robot is straight movement but a forward direction with a low actuation frequency lower than 8 Hz and a reverse direction with a relatively high actuation frequency higher than 8 Hz. Moreover, the steering of the robot can also be achieved by a different stride length between its two legs. For instance, when the stride length of the right leg is larger than the left one, the robot will turn to the left.

Then, we further demonstrate how this dexterous amphibious robot efficiently accomplishes more complex tasks by self-sensing adaption without any external support. The first scenario is self-adaptive obstacle avoidance. Figure 5C shows the complete avoidance process between the robot and the obstacle (Video S5 and more in Text S5), which can be divided into three stages in time sequence.

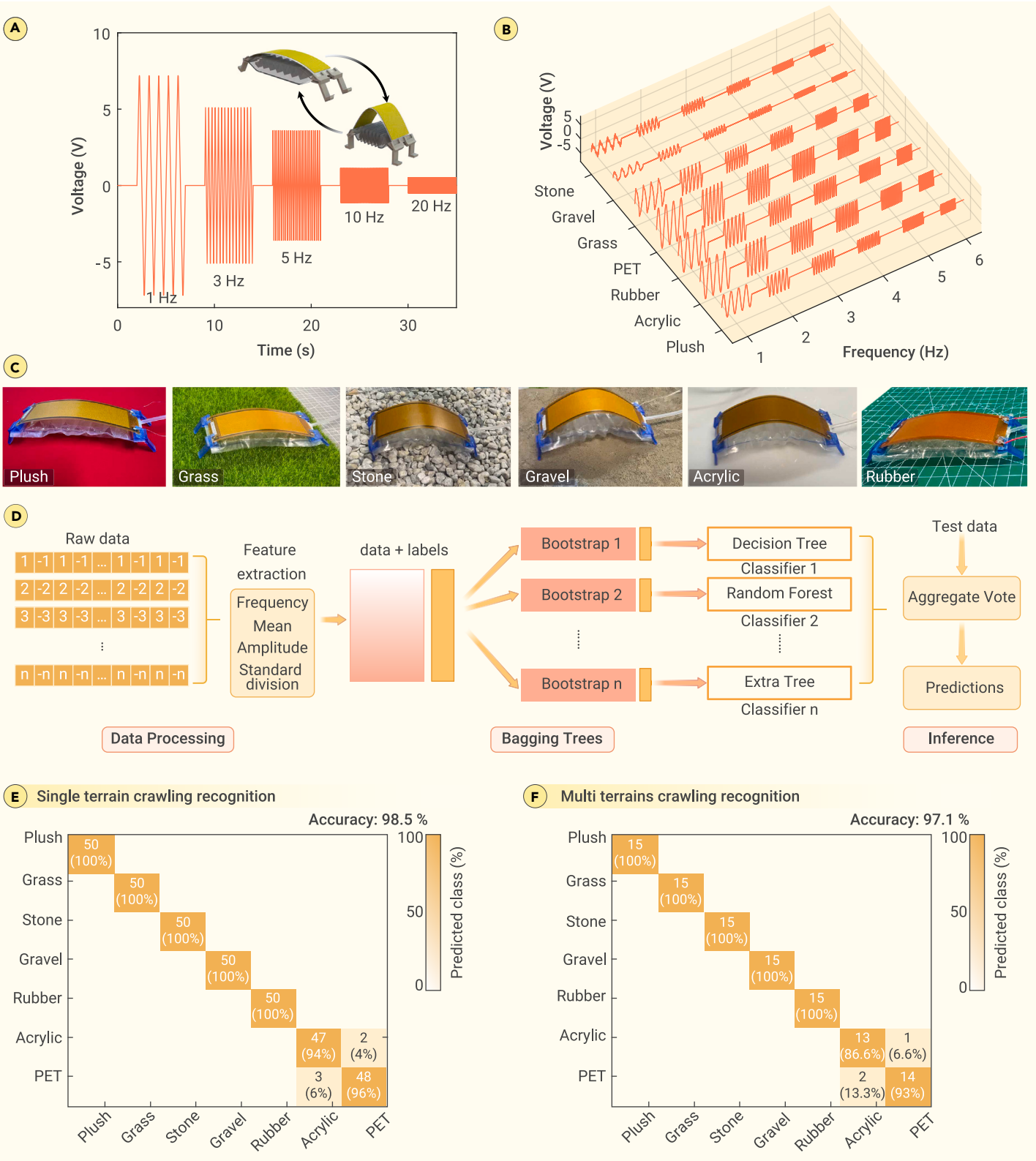

Figure 3. Environmental awareness and recognition by the spinal robot (A) Measured feedback signal by the spine when the robot moves with an increased actuation frequency from 1 Hz to 20 Hz. (B) Measured feedback signal of the spine when the robot crawls on different terrains as a function of actuation frequency. (C) Images of the crawling robot on different terrains, including some relatively smooth terrains, i.e., rubber land, PET land, acrylic land, and plush land, and some uneven terrains, i.e., grass land, gravel land, and stone land. (D) Flow diagram of the machine learning process. (E) Classification confusion matrix of the robotic recognition on single-terrain tasks, with an overall accuracy of 98%. (F) Classification confusion matrix of the robotic recognition on multi-terrain tasks, with an overall accuracy of 97.1%.

(1) The robot moves forward to approach the obstacle and collides with it (from 0 s to 6 s, with an actuation frequency of 1 Hz); (2) the robot detects the obstacle in its path and makes a decision to walk around it, followed by self-adjusted motion state to reverse and move away from the obstacle (from 6 s to 13 s, with an actuation frequency of 8 Hz); and (3) the robot adjusts its pathway and steers to avoid the obstacle (from 13 s to 31 s, with an actuation frequency of 2 Hz). Figure 5C also shows the actuation signals for both of the robotic legs during the whole process. As we mentioned above, this self-adaptive obstacle avoidance is independent from external devices and vision, so it fully demonstrates the active intelligence of the robotic design and is still available in dark environments.

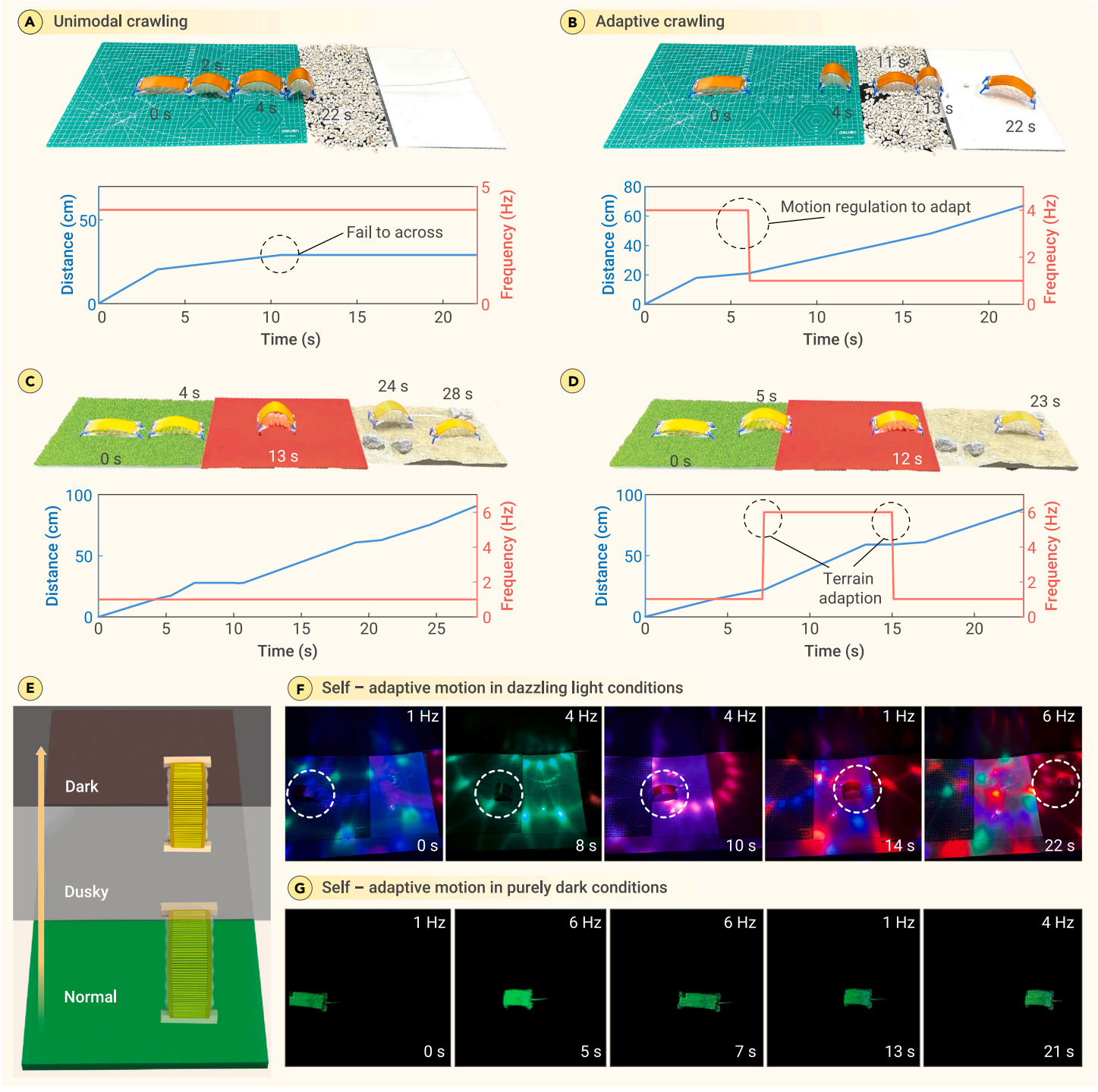

Figure 4. Self-sensing adaption by the spinal robot in multi-terrain tasks (A and C) The unimodal crawling robot moves over two multi-terrains scenarios, as the first scenario (A) contains rubber land, stone land, and PET land, and the second scenario (C) contains grass land, plush land, and gravel land. (B) The spinal crawling robot with self-sensing adaption for the first scenario, overcoming the terrain boundary that the unimodal one failed. (D) The spinal crawling robot for the second scenario, showing it to be 18% faster than the unimodal one. (E) Self-sensing adaption of the spinal robot remains available in dusky and dark environments. (F) Images of the spinal crawling robot performing a self-adaptive multi-terrain-crossing task in dazzling light condition. (G) Images of the spinal crawling robot performing another self-adaptive crossing task in purely dark condition.

The second scenario is self-adaptive amphibious motion, which contains multiple environments at different altitudes, including gravel land, grass land, soil descent, and aquatic area (Video S6). As shown in Figure 5D, we divide the whole self-adaptive motion of the amphibious robot into three stages in time sequences. (1) The robot moves forward and performs self-adaptive multi-terrain transitions between plush land, gravel land, and the grass land (from 0 s to 15 s); (2) the robot undergoes a soil descent and gradually moves closer to the aquatic area (from 16 s to 25 s, with an actuation frequency of 2 Hz); and (3) the robot adapts to the aquatic area to swim efficiently (from 26 s to 33 s, with a self-adjusted frequency of 4 Hz). The self-sensing adaptability has resulted in a 22% improvement in overall time when moving across this land-aquatic path compared to the unimodal robot (Figures S19 and S20).

CONCLUSION

In summary, we have shown that a unibody sensor-actuator-integrated spine provides a potential for high-level intelligence for soft robots. As the core component in our proposal, a piezoelectric macro-fiber composite sheet acts as a bionic spine for both perception and auxiliary actuation, facilitating a synergistic and complementary action between the sensor and actuator. More importantly, we demonstrate that this highly intelligent

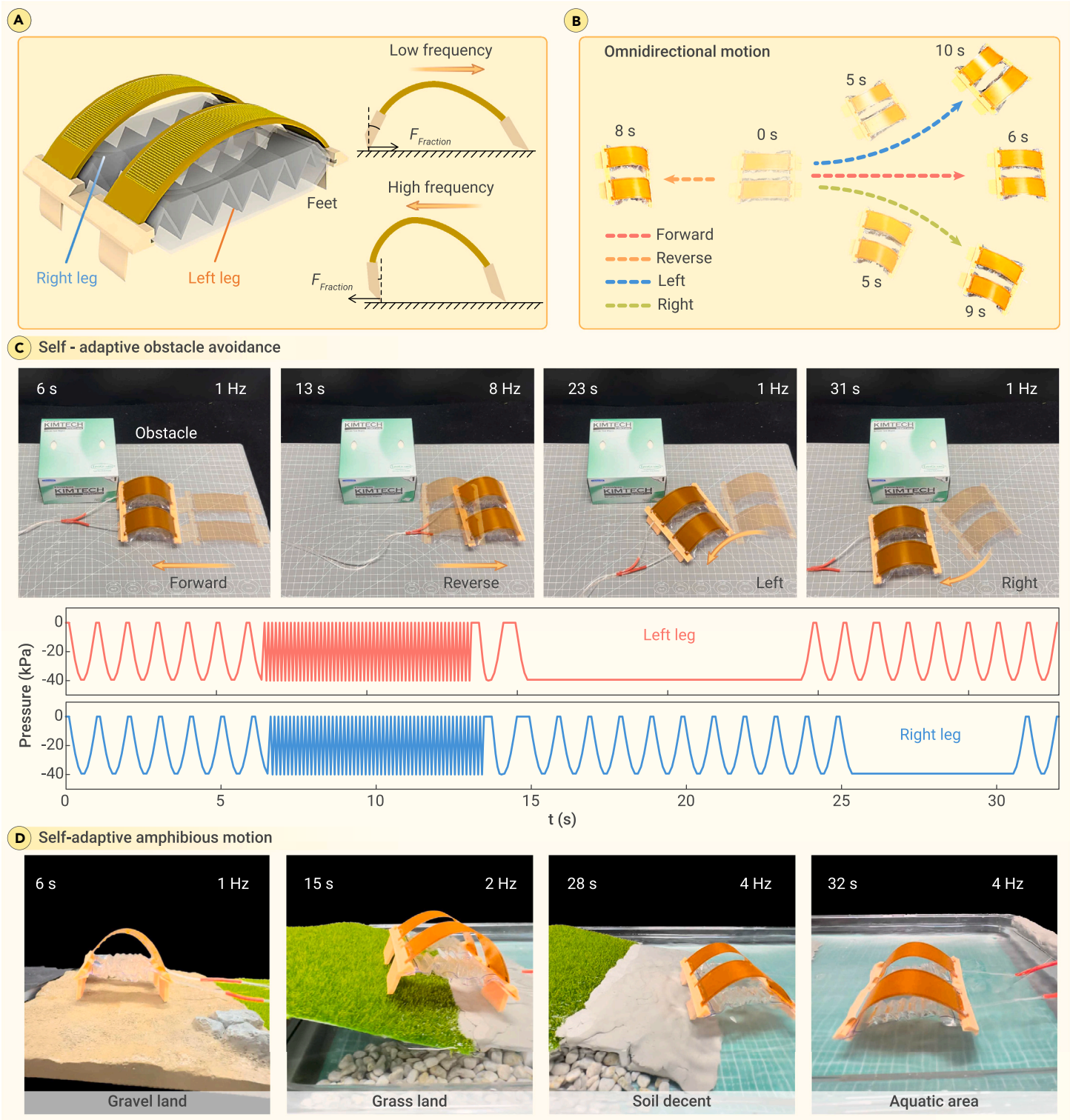

Figure 5. An amphibious and omnidirectional spinal soft robot (A) Design and reversible locomotive mechanism of the robot consisting of twin actuators in parallel. (B) Omnidirectional motions of the robot. (C) Images of the robot performing a self-adaptive obstacle avoidance with self-sensing adaption and dexterous motion. (D) Images of the robot performing multi-terrain crossing and amphibious transition with self-sensing adaption.

soft robot can accomplish beyond-biological applications with vision-free self-sensing adaption, including efficient multi-terrain transition, obstacle avoidance, and amphibious locomotion.

Although there is clearly excellent environmental compatibility and decision-making capacity, the performance of this proposed soft robot still lags behind advanced vertebrate animals, in terms of agility, responsiveness, etc. This is mainly due to the limitations of soft materials and robotic perception systems, causing a worse overall responsive speed compared to vertebrates. Therefore, a dexterous and robust soft actuator with highly sensitive perception is desired to construct a more advanced version based upon this work for broader deployments. Our approach is the first to promote the synergy between sensor and actuator components to implement autonomous adaption, and this could spark future innovations for high-level intelligent soft robots.

MATERIALS AND METHODS

See supplemental information for details.

REFERENCES

1. Rus, D., and Tolley, M.T. (2015). Design, fabrication and control of soft robots. Nature ***521***(7553): 467–475. https://doi.org/10.1038/nature14543.
2. Xiong, J., Chen, J., and Lee, P.S. (2021). Functional Fibers and Fabrics for Soft Robotics, Wearables, and Human-Robot Interface. Adv. Mater. ***33***(19): 2002640. https://doi.org/10.1002/adma.202002640.
3. Han, C., Jeong, Y., Ahn, J., et al. (2023). Recent Advances in Sensor-Actuator Hybrid Soft Systems: Core Advantages, Intelligent Applications, and Future Perspectives. Adv. Sci. ***10***: 2302775. https://doi.org/10.1002/advs.202302775.
4. Li, G., Chen, X., Zhou, F., et al. (2021). Self-powered soft robot in the Mariana Trench. Nature ***591***(7848): 66–71. https://doi.org/10.1038/s41586-020-03153-z.
5. Li, M., Pal, A., Aghakhani, A., et al. (2022). Soft actuators for real-world applications. Nat. Rev. Mater. ***7***(3): 235–249. https://doi.org/10.1038/s41578-021-00389-7.
6. Kim, S., Laschi, C., and Trimmer, B. (2013). Soft robotics: a bioinspired evolution in robotics. Trends Biotechnol. ***31***(5): 287–294. https://doi.org/10.1016/j.tibtech.2013.03.002.
7. Zhang, Y., Zhang, W., Gao, P., et al. (2022). Finger-palm synergistic soft gripper for dynamic capture via energy harvesting and dissipation. Nat. Commun. ***13***(1): 7700. https://doi.org/10.1038/s41467-022-35479-9.
8. Ma, K., Chen, X., Zhang, J., et al. (2023). Inspired by Physical Intelligence of an Elephant Trunk: Biomimetic Soft Robot With Pre-Programmable Localized Stiffness. IEEE Rob. Autom. Lett. ***8***(5): 2898–2905. https://doi.org/10.1109/LRA.2023.3256922.
9. Yao, T., Kos, Ž., Zhang, Q.X., et al. (2022). Nematic Colloidal Micro-Robots as Physically Intelligent Systems. Adv. Funct. Mater. ***32***(44): 2205546. https://doi.org/10.1002/adfm.202205546.
10. Hausladen, M.M., Zhao, B., Kubala, M.S., et al. (2022). Synthetic growth by self-lubricated photopolymerization and extrusion inspired by plants and fungi. Proc. Natl. Acad. Sci. USA ***119***(33): e2201776119. https://doi.org/10.1073/pnas.2201776119.
11. Zhao, Y., Chi, Y., Hong, Y., et al. (2022). Twisting for soft intelligent autonomous robot in unstructured environments. Proc. Natl. Acad. Sci. USA ***119***(22): e2200265119. https://doi.org/10.1073/pnas.2200265119.
12. Sun, J., Lerner, E., Tighe, B., et al. (2023). Embedded shape morphing for morphologically adaptive robots. Nat. Commun. ***14***(1): 6023. https://doi.org/10.1038/s41467-023-41708-6.
13. Baines, R., Patiballa, S.K., Booth, J., et al. (2022). Multi-environment robotic transitions through adaptive morphogenesis. Nature ***610***(7931): 283–289. https://doi.org/10.1038/s41586-022-05188-w.
14. Ilami, M., Bagheri, H., Ahmed, R., et al. (2021). Materials, Actuators, and Sensors for Soft Bioinspired Robots. Adv. Mater. ***33***(19): 2003139. https://doi.org/10.1002/adma.202003139.
15. Gu, G., Zhang, N., Xu, H., et al. (2023). A soft neuroprosthetic hand providing simultaneous myoelectric control and tactile feedback. Nat. Biomed. Eng. ***7***(4): 589–598. https://doi.org/10.1038/s41551-021-00767-0.
16. Dai, J., Li, X.-G., Zhang, T.-Y., et al. (2024). Illuminating a bacterial adaptation mechanism: Infrared-driven cell division in deep-sea hydrothermal vent environments. The Innovation Geoscience ***2***(1): 100050. https://doi.org/10.59717/j.xinn-geo.2024.100050.
17. Tan, D., and Xu, B. (2023). Advanced Interfacial Design for Electronic Skins with Customizable Functionalities and Wearability. Adv. Funct. Mater. ***33***: 2306793. https://doi.org/10.1002/adfm.202306793.
18. Peng, X., Dong, K., Ye, C., et al. (2020). A breathable, biodegradable, antibacterial, and self-powered electronic skin based on all-nanofiber triboelectric nanogenerators. Sci. Adv. ***6***(26): eaba9624. https://doi.org/10.1126/sciadv.aba9624.
19. Zou, Z., Zhu, C., Li, Y., et al. (2018). Rehealable, fully recyclable, and malleable electronic skin enabled by dynamic covalent thermoset nanocomposite. Sci. Adv. ***4***(2): eaaq0508. https://doi.org/10.1126/sciadv.aaq0508.
20. Park, J., Kim, D., and Kim, Y.T. (2021). Soft and transparent triboelectric nanogenerator based E-skin for wearable energy harvesting and pressure sensing. Nanotechnology ***32***(38): 385403. https://doi.org/10.1088/1361-6528/ac0c3f.
21. Guo, N., Han, X., Liu, X., et al. (2023). Autoencoding a Soft Touch to Learn Grasping from On-Land to Underwater. Adv. Intell. Syst. ***6***(3): 2200269. https://doi.org/10.1002/aisy.202300382.
22. Wang, X., Fang, G., Wang, K., et al. (2020). Eye-in-Hand Visual Servoing Enhanced With Sparse Strain Measurement for Soft Continuum Robots. Autom. Lett. ***5***(2): 2161–2168. https://doi.org/10.1109/LRA.2020.2969953.
23. Liu, X., Onal, C.D., and Fu, J. (2023). Reinforcement Learning of CPG-Regulated Locomotion Controller for a Soft Snake Robot. IEEE Trans. Robot. ***39***(5): 3382–3401. https://doi.org/10.1109/TRO.2023.3286046.
24. Hawkes, E.W., Blumenschein, L.H., Greer, J.D., et al. (2017). A soft robot that navigates its environment through growth. Sci. Robot. ***2***(8): eaan3028. https://doi.org/10.1126/scirobotics.aan3028.
25. Huang, C., Xu, T., Liu, J., et al. (2019). Visual Servoing of Miniature Magnetic Film Swimming Robots for 3-D Arbitrary Path Following. IEEE Rob. Autom. Lett. ***4***(4): 4185–4191. https://doi.org/10.1109/LRA.2019.2931234.
26. Xu, F., Wang, H., Liu, Z., et al. (2022). Visual Servoing Pushing Control of the Soft Robot with Active Pushing Force Regulation. Soft Robot. ***9***(4): 690–704. https://doi.org/10.1089/soro.2020.0178.
27. Yang, X., Lan, L., Pan, X., et al. (2023). Bioinspired soft robots based on organic polymer-crystal hybrid materials with response to temperature and humidity. Nat. Commun. ***14***(1): 2287. https://doi.org/10.1038/s41467-023-37964-1.
28. Wang, C., Wu, Y., Dong, X., et al. (2023). In situ sensing physiological properties of biological tissues using wireless miniature soft robots. Sci. Adv. ***9***(23): eadg3988. https://doi.org/10.1126/sciadv.adg3988.
29. Su, Q., Zou, Q., Li, Y., et al. (2021). A stretchable and strain-unperturbed pressure sensor for motion interference–free tactile monitoring on skins. Sci. Adv. ***7***(48): eabi4563. https://doi.org/10.1126/sciadv.abi4563.
30. Lin, W., Zhang, D., Lee, W.W., et al. (2022). Super-resolution wearable electrotactile rendering system. Sci. Adv. ***8***(36): eabp8738. https://doi.org/10.1126/sciadv.abp8738.
31. Li, D., Zhou, J., Yao, K., et al. (2022). Touch IoT enabled by wireless self-sensing and haptic-reproducing electronic skin. Sci. Adv. ***8***(51): eade2450. https://doi.org/10.1126/sciadv.ade2450.
32. Liu, W., Duo, Y., Liu, J., et al. (2022). Touchless interactive teaching of soft robots through flexible bimodal sensory interfaces. Nat. Commun. ***13***(1): 5030. https://doi.org/10.1038/s41467-022-32702-5.
33. Jiang, S., Zhang, T., Zhou, Y., et al. (2023). Wearable ultrasound bioelectronics for healthcare monitoring. Innovation ***4***(4): 100447. https://doi.org/10.1016/j.xinn.2023.100447.
34. Zhang, T., Liu, N., Xu, J., et al. (2023). Flexible electronics for cardiovascular healthcare monitoring. Innovation ***4***(5): 100485. https://doi.org/10.1016/j.xinn.2023.100485.
35. Shahsavan, H., Aghakhani, A., Zeng, H., et al. (2020). Bioinspired underwater locomotion of light-driven liquid crystal gels. Proc. Natl. Acad. Sci. USA ***117***(10): 5125–5133. https://doi.org/10.1073/pnas.1917952117.
36. Truby, R.L., Santina, C.D., and Rus, D. (2020). Distributed Proprioception of 3D Configuration in Soft, Sensorized Robots via Deep Learning. IEEE Rob. Autom. Lett. ***5***(2): 3299–3306. https://doi.org/10.1109/LRA.2020.2976320.
37. Jin, L., Li, Z., Liu, Z., et al. (2022). Flexible unimodal strain sensors for human motion detection and differentiation. npj Flex. Electron. ***6***(1): 74. https://doi.org/10.1038/s41528-022-00205-4.
38. Kim, M., Yu, A., Kim, D., et al. (2023). Multi-Agent Control of Laser-Guided Shape-Memory Alloy Microrobots. Adv. Funct. Mater. ***33***: 2304937. https://doi.org/10.1002/adfm.202304937.
39. Hu, D., Giorgio-Serchi, F., Zhang, S., et al. (2023). Stretchable e-skin and transformer enable high-resolution morphological reconstruction for soft robots. Nat. Mach. Intell. ***5***(3): 261–272. https://doi.org/10.1038/s42256-023-00622-8.
40. Shih, B., Shah, D., Li, J., et al. (2020). Electronic skins and machine learning for intelligent soft robots. Sci. Robot. ***5***(41): eaaz9239. https://doi.org/10.1126/scirobotics.aaz9239.
41. Liu, W., Duo, Y., Chen, X., et al. (2023). An Intelligent Robotic System Capable of Sensing and Describing Objects Based on Bimodal, Self-Powered Flexible Sensors. Adv. Funct. Mater. ***33***(41): 2306368. https://doi.org/10.1002/adfm.202306368.
42. Deng, M., Fan, F., and Wei, X. (2023). Learning-Based Object Recognition via a Eutectogel Electronic Skin Enabled Soft Robotic Gripper. IEEE Rob. Autom. Lett. ***8***(11): 7424–7431. https://doi.org/10.1109/LRA.2023.3316096.
43. Thuruthel, T.G., Shih, B., Laschi, C., et al. (2019). Soft robot perception using embedded soft sensors and recurrent neural networks. Sci. Robot. ***4***(26): eaav1488. https://doi.org/10.1126/scirobotics.aav1488.
44. Jin, T., Sun, Z., Li, L., et al. (2020). Triboelectric nanogenerator sensors for soft robotics aiming at digital twin applications. Nat. Commun. ***11***(1): 5381. https://doi.org/10.1038/s41467-020-19059-3.
45. Xie, M., Zhu, M., Yang, Z., et al. (2021). Flexible self-powered multifunctional sensor for stiffness-tunable soft robotic gripper by multimaterial 3D printing. Nano Energy ***79***: 105438. https://doi.org/10.1016/j.nanoen.2020.105438.
46. Gong, S., Ding, Q., Wu, J., et al. (2022). Bioinspired Multifunctional Mechanoreception of Soft–Rigid Hybrid Actuator Fingers. Adv. Intell. Syst. ***4***(5): 2100242. https://doi.org/10.1002/aisy.202100242.
47. Yan, H., Wang, Y., Shen, W., et al. (2022). Cable-Driven Continuum Robot Perception Using Skin-Like Hydrogel Sensors. Adv. Funct. Mater. ***32***(34): 2203241. https://doi.org/10.1002/adfm.202203241.
48. Jiao, Z., Hu, Z., Shi, Y., et al. (2024). Reprogrammable, intelligent soft origami LEGO coupling actuation, computation, and sensing. Innovation ***5***(1): 100549. https://doi.org/10.1016/j.xinn.2023.100549.

ACKNOWLEDGMENTS

This work was supported by the National Natural Science Foundation of China, China (12102250 and 12032015), the Science and Technology Innovation Action Plan of Shanghai, China (21190760100) the Medical Engineering Interdisciplinary Research Fund for "Star of Jiao Tong University" of Shanghai Jiao Tong University, China, and the Oceanic Interdisciplinary Program of Shanghai Jiao Tong University (SL2023MS006)

AUTHOR CONTRIBUTIONS

S.G. and F.F. initiated the concept with the help of Z.Y., L.S., and W.Z. S.G. and F.F. designed and performed all the experiments under the guidance of Z.Y., L.S., and W.Z., with help from A.L., B.F., and W.L. S.G. wrote the initial manuscript, which was revised by Z.Y. L.S. and W.Z. supervised the project and provided funding. All authors contributed to the discussion and writing of this manuscript.

DECLARATION OF INTERESTS

The authors declare no competing interests.

SUPPLEMENTAL INFORMATION

It can be found online at https://doi.org/10.1016/j.xinn.2024.100640.

LEAD CONTACT WEBSITE

https://me.sjtu.edu.cn/teacher_directory1/zhangwenming.html.